SASEC2015
Third Southern African Solar Energy Conference
11 – 13 May 2015
Kruger National Park, South Africa

EFFECT OF METAL MATRIX AND FOAM POROSITY ON THERMAL PERFORMANCE OF LATENT HEAT THERMAL STORAGE FOR SOLAR THERMAL POWER PLANT

S Halder[a], S Singh[a], S K Saha[b,*]
[a]Department of Energy Science and Engineering, Indian Institute of Technology Bombay, Powai, Mumbai- 400076, INDIA.
[b]Department of Mechanical Engineering, Indian Institute of Technology Bombay, Powai, Mumbai- 400076, INDIA.
* Corresponding author. Tel.: +91 22 25767392; fax: +91 22 2572 6875.
E-mail address: sandip.saha@iitb.ac.in

ABSTRACT

In this paper, the thermal performance of latent heat thermal storage system using metal matrix and foam is investigated for the medium temperature (~ 200 ^{0}C) and medium power (~1 MW) ORC-based solar thermal power plant. The latent heat storage system using phase change materials (PCMs) is an effective way of storing thermal energy and has the advantage of high-energy storage density which makes the storage system compact. The main drawback of PCMs like molten salts is its low thermal conductivity (~0.2-0.5 W/m.K) which inhibits heat transfer to/from PCM. To overcome this, metal matrix and foam are introduced in PCM as thermal conductivity enhancers (TCE) to improve the heat transfer rate. The volume averaging technique for porous medium is adopted to model the metal foam and matrix embedded in PCM. The fluid flow and phase change in porous medium is modelled using single domain enthalpy–porosity technique. A parametric study is performed to show the effect of porosity of the metal matrix and foam on the outlet temperature of heat transfer (HTF) during charging/ discharging period. It is found that the TES with 0.7 metal matrix and foam porosity performs better than TES with PCM and any other porosity.

INTRODUCTION

The short-term storage of thermal energy at low or high temperatures in a medium can be defined as thermal energy storage (TES). The TES has been used for decades and it is an important component of the power generating plant, especially, if the energy supply is irregular. The intermittent, variable and unpredictable nature of solar radiation generally leads to a mismatch between the rate at the time of collection and the time of supply of solar energy. Hence, there is a need to use a storage system [1]. By smoothing supply, increasing reliability and levelling the load, a TES can improve the performance of a power generating plant. The storage system stores energy when the collected amount is in excess of the requirement of the application and discharges energy when the supply is inadequate. The size of a storage system is largely determined by the specific purpose for which it is used. Another significant characteristic of a TES is its volumetric energy storage capacity which governs its size. The storage system would be better if the volume is smaller that reduces the installation space requirement. Therefore a good storage system should have more energy storage capacity per unit volume and a long storage time [1]. In this context, latent heat thermal energy storage (LHTES) using phase change material (PCM) can be used, as PCM possesses high latent heat of melting. LHTS provides high-energy storage density and it can store heat at constant temperature corresponding to the phase transition temperature of PCM relative to the sensible energy storage. A PCM based TES plays a major role in energy conservation, minimizes the disparity between the demand and the supply and also improves the performance and reliability of the storage system. Particularly PCMs are much more useful than sensible storage where the temperature difference between the source and the sink is low.

NOMENCLATURE

a_{sf}	[m^{-1}]	Interfacial surface area
A_b	[m^2]	Exposed area of base of fins
A_c	[m^2]	Cross sectional area of fin
A_f	[m^2]	Fin surface area
A_i	[m^2]	Area of the inner pipe
A_t	[m^2]	Fin surface area + exposed portion of base
c_p	[J/kg.K]	Specific heat
C	[-]	Inertial coefficient
$C_{D,f}$	[-]	Drag coefficient
d_i	[m]	Inner diameter of HTF flowing pipe
d_o	[m]	Outer diameter of HTF flowing pipe
d_p	[m]	Pore diameter
d_{fi}	[m]	Fibre diameter
D_i	[m]	Inner diameter of the TES
E	[J/kg]	Enthalpy
f_l	[-]	Liquid fraction
g	[m/s^2]	Acceleration due to gravity
h	[W/m^2 K]	Heat transfer coefficient
h_{sf}	[W/m^2 K]	Interfacial heat transfer coefficient in porous medium
H	[m]	Height

k	[W/mK]	Thermal conductivity
k_f	[W/mK]	Thermal conductivity of fin material
K	[-]	Permeability
L	[m]	Length
L_{latent}	[J/kgK]	Latent heat of fusion
$\dot{m}$	[kg/s]	Mass flow rate of HTF
N	[-]	Number of fins inside the HTF tubes
Nu	[-]	Nusselt number
$\dot{Q}$	[W]	Heat transfer rate
r,θ,z	[-]	Coordinates
Re	[-]	Reynolds number
R	[mK/W]	Thermal resistance per unit length
$R_{f,o}$	[mK/W]	Overall fin resistance per unit length
S	[-]	Source term
t	[s]	Time
t_{charge}	[s]	Charging period
t_f	[m]	Thickness of fin
T	[°C]	Temperature
$T_{surface}$	[°C]	Surface temperature of TES
u_r,u_θ,u_z	[m/s]	Velocity component in *r, θ and z* directions
V_{PCM}	[m³]	Total volume of PCM

Special characters

α	[m^2/s]	Thermal diffusivity
β	[K^{-1}]	Thermal expansion coefficient
η_f	[-]	Fin efficiency
η_o	[-]	Overall fin efficiency
ΔE	[J/kg]	Nodal latent heat
ε	[-]	Liquid phase fraction
μ	[kg/ms]	Dynamic viscosity
ν	[m²/s]	Kinematic viscosity
ρ	[kg/m³]	Density
Ψ	[-]	Tortuosity
δ	[-]	Porosity

Subscripts

eff	Effective value
f	PCM phase
i	Inner
in	Inlet
li	Liquid
m	Melting point
o	Outer
out	Outlet
s	Solid

However the main drawback of PCM is its low thermal conductivity [2] which results in low charging and discharging rates that cause a decrease in the overall efficiency of the system [3]. To overcome this, heat transfer enhancement techniques are required such as insertion of metal matrix into the PCM [4], using PCM dispersed with high conductivity particles [5], micro-encapsulation of PCM [6], using shell and tube arrangements [7] or finned tube of different configurations.

Literatures exist on various configurations, however the most intensely analysed LHTES unit is the shell and tube system, accounting for more than 70% [8]. Mesalhy et al. [9] developed a numerical model to study the effect of adding a high thermal conductivity matrix on the performance of the PCM based TES. They found that the heat transfer and melting rate of the PCM energy storage augment by inserting the porous matrix in the PCM. The melting rate of PCM can be increased by decreasing the porosity of the matrix as the conduction heat transfer is more dominant. The thermal conductivity of metal matrix plays an important role on the response of the PCM storage. From the literature review, it can be concluded that researchers studied various techniques for enhancing the thermal conductivity of PCM for the low temperature application (< 100 °C). For medium or high temperature applications (> 100°C), these enhancement techniques are required to be explored. Also there is a need for a systematic study to evaluate the thermal performance of the phase change material (PCM) based thermal energy storage system using the thermal conductivity enhancers.

In this paper, the thermal performance of a thermal energy storage system (TES) using phase change material (PCM) is investigated numerically for the medium temperature organic Rankine cycle (ORC) based solar thermal power plant (~ 200 °C) under fluctuating inlet condition of heat transfer fluid (HTF) to the power generating unit such as turbine or heat exchanger. To remove the temperature fluctuation in HTF and to maintain the efficiency of solar thermal power plant at a desire level, a PCM-based thermal storage system is placed between the solar collector and the turbine or the heat exchanger. A cycle comprising of charging and discharging period of 1800 s each is considered to represent fluctuations in the inlet temperature of HTF. During charging and discharging period, the inlet temperature of HTF is taken as (T_{in}) 200 and 132 °C, respectively. Based on the requirement of the HTF temperature to be maintained at 166 ^{0}C, an eutectic mixture of $LiNO_3$ (58.1 by mol %) and KCl (41.9 by mol %) having an isothermal melting temperature of 166 ^{0}C is chosen as PCM. The HTF is selected as Hytherm 600. The container material is selected as 304 stainless steel with Teflon coating to reduce corrosion due to molten salt. Based on the objective, a PCM-based thermal storage system is designed first analytically. A numerical model taking into account of the phase change behaviour is developed to characterize the storage system. Metal foam and matrix is used as the thermal conductivity enhancers (TCE) in the present study. The heat transfer enhancement of PCM with TCE in TES is further evaluated and compared with the base case, which is, TES filled with PCM. The effect of porosity of metal foam and matrix on the thermal performance of PCM-based TES is also investigated.

PRELIMINARY DESIGN OF A PCM-BASED TES

The preliminary design of a LHTES for charging period is performed by considering one dimensional steady state conduction heat transfer. In the designing of thermal energy storage unit, it is considered that the phase change material (PCM) is at the melting temperature initially, however in solid state. Due to application of heat to TES during charging period, PCM will start melting isothermally and change its state to liquid. During phase change, PCM will maintain the fluctuating temperature of the incoming heat transfer fluid (HTF) at a certain level. The cylindrical configuration is chosen as a basic configuration of the TES and is shown in figure 1. The thermophysical properties of Hytherm 600 and the eutectic mixture of $LiNO_3$ (58.1 by mol %) and KCl (41.9 by mol %) are listed in table 1. The thermal expansion coefficient (β) and the latent heat (L_{latent}) of PCM are taken as 0.00066 K^{-1} and 272 kJ/kg, respectively.

The volume (V_{PCM}) of TES containing PCM can be found as,

$$\dot{Q}t_{charge} = \rho_{PCM}V_{PCM}L_{latent} \quad (1)$$

The charging period (t_{charge}) is taken as 1800 seconds. The inner diameter (D_i) of the TES can be calculated as,

$$D_i = \sqrt{\frac{4V_{PCM}}{\pi L} + d_i^2} \quad (2)$$

The inner diameter (d_i) of pipe through which HTF is flowing is taken as 10.4 mm with the outer diameter (d_o) corresponds to 13.7 mm. For simplicity, the thickness of the pipe is neglected and the inner diameter of pipe is considered in the calculations. Therefore the inner diameter (D_i) of TES can be calculated from equation 2, if V_{PCM} and L are known. To calculate the dimensions of TES, the following expression is written by considering the energy balance between HTF and PCM,

$$\dot{Q} = \dot{m}c_p(T_{in} - T_{out}) = \frac{(T_{mean} - T_{htf,o})}{\left(\frac{1}{hA_i}\right)} = \frac{(T_{htf,o} - T_{surface})}{\frac{ln\left(\frac{D_i}{d_i}\right)}{2\pi k_{PCM} L}} \quad (3)$$

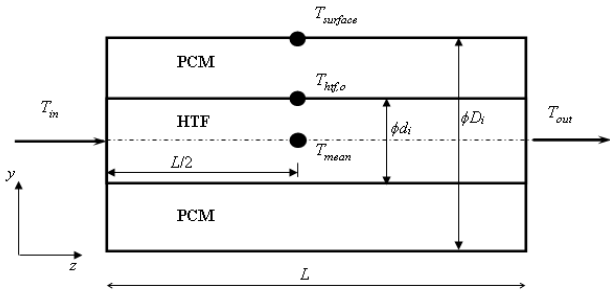

Figure 1 Cylindrical thermal energy storage unit of L = 800 mm

For given mass flow rate ($\dot{m} = 0.00295\ kg/s$), inlet HTF temperature ($T_{in} = 200$ ℃) and outlet HTF temperature ($T_{out} = 166$ ℃), the required storage capacity $(\dot{Q})$ is calculated as 310.7 W. By trial and error method, the length (L) of the TES is found as 13 m for a single pass from equation 3 assuming $T_{surface} = 166$ °C. The outer diameter of TES is obtained as 14.4 mm.

The length of the TES can be reduced by incorporating fins in the inner pipe through which HTF is flowing as the addition of fins will reduce the thermal resistance of HTF (R_{HTF}). As the fins are aligned along the direction of HTF flow, the losses will be negligible. The fin and container are made of SS 304 and its thermophysical properties are tabulated in table 1.

Table 1 Theromophysical properties of Materials

Material	P	c_p	k	μ	T_m
HTF	720.9	3097.4	0.116	0.0195	-
PCM	2010	1485	0.5	0.003	166
Steel 304	8030	502.48	16	-	-

The resistance of HTF (R_{HTF}) can be found by calculating the overall fin resistance, which is given as,

$$R_{f,o} = \frac{1}{\eta_o h A_t} \quad (4)$$

where the overall fin efficiency can be determined as,

$$\eta_o = \left[1 - \frac{NA_f}{A_t}(1 - \eta_f)\right] \quad (5)$$

where the fin efficiency is given by,

$$\eta_f = \frac{tanh(mH_c)}{mH_c} \quad (6)$$

where H_c is corrected fin height that can be written as,

$$H_c = H + \frac{t_f}{2} \quad (7)$$

In equation (6), m is calculated as,

$$m = \sqrt{\frac{hP}{k_f A_c}} \quad (8)$$

and mH_c is taken as 0.31. The ratio of fin perimeter to its cross sectional area for a slender fin ($t \ll L_f$) can be written as,

$$\frac{P}{A_c} = \frac{2}{t} \quad (9)$$

The total number of fins (N) is taken as 6 and the thickness of a fin (t_f) is considered as 1 mm. Therefore, the length (L) of TES is reduced to 5.6 m for a single pass with the addition of fins. For multipass of HTF pipes in TES, the length of the TES is estimated as 0.8 m for 7 parallel HTF flowing tubes and the outer diameter (D_i) of TES is found as 68 mm. Figure 2 shows the schematic diagram of the TES without fins inside HTF tubes. An enlarged view of a HTF pipe with 6 fins is shown in figure 3.

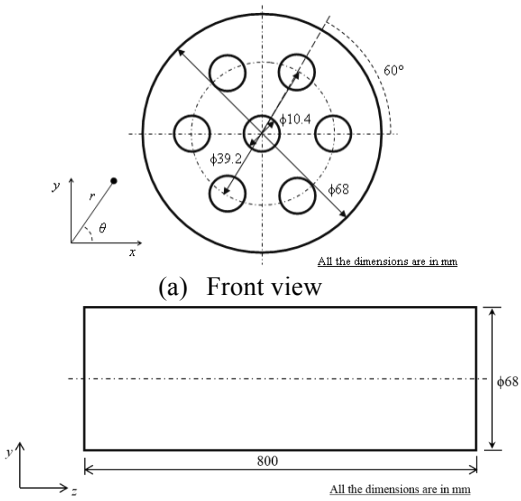

Figure 2 (a) Front view and (b) side view of the LHTES with fins inside the HTF tubes

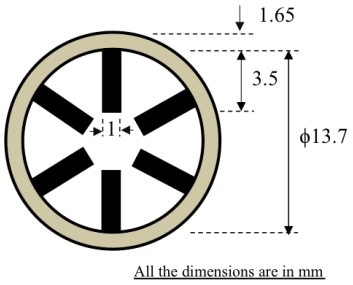

Figure 3 Schematic diagram of a HTF flowing pipe with internal fins

NUMERICAL DOMAIN

The PCM-based TES can be divided into 6 symmetric parts and the thermal behaviour of the TES can be represented by one part as it is symmetric with the others. Figure 4 shows the numerical domain of L = 800 mm chosen for the simulation. The inner diameter (D_i) of TES is taken as 100 mm which is greater than the calculated one to accommodate the thermal conductivity enhancers (TES) such as metal matrix and foam. The two-dimensional analysis is not adequate for the numerical domain shown in figure 4, hence three-dimensional modelling is adopted in the numerical simulations. The direction of g is taken along the flow through tubes as shown in the figure.

Governing Equations

The metal matrix and foam are numerically modelled as a porous medium. The volume averaging technique for porous medium is adopted to model the metal foam and matrix embedded in PCM. The fluid flow and phase change in porous medium is modelled using single domain enthalpy–porosity technique [10]. For the present model, phase change is assumed to be isothermal. Assuming isotropic porosity and single phase flow, the governing partial differential equations describing the melting of the PCM inside the porous matrix are obtained from volume-averaging of the mass, momentum and energy conservation equations [9]. There are large differences in thermal properties between the PCM and the metal matrix. Hence a two-energy equations model is adopted to solve the energy conservation equations. This model can handle the local thermal non-equilibrium condition between the PCM and the metal matrix. The properties of PCM and metal matrix are assumed to be constant and it is also assumed that there is no volume change during the melting process. The equivalent governing equations in the vector form are given by:

Conservation of mass:

$$\frac{\partial \rho_p}{\partial t} + \nabla.\left(\rho_p V\right) = 0 \tag{10}$$

Conservation of momentum:

$$\frac{1}{\varepsilon}\frac{\partial(\rho_p V)}{\partial t} + \frac{1}{\varepsilon^2}\nabla.\left(\rho_p V\, V\right) = -\nabla p + \nabla.\left(\frac{\mu}{\varepsilon}\nabla V\right) + S_i \tag{11}$$

PCM energy equation:

$$\delta\frac{\partial(\rho_p c_{pf} T_f)}{\partial t} + \nabla.\left(\rho_p c_{pf} V T_f\right) = \nabla.\left(k_{e,eff}\nabla T_f\right) + S_{Tf} \tag{12}$$

Solid matrix energy equation:

$$(1-\delta)\frac{\partial(\rho_s c_{ps} T_s)}{\partial t} = \nabla.\left(k_{s,eff}\nabla T_s\right) + S_{Ts} \tag{13}$$

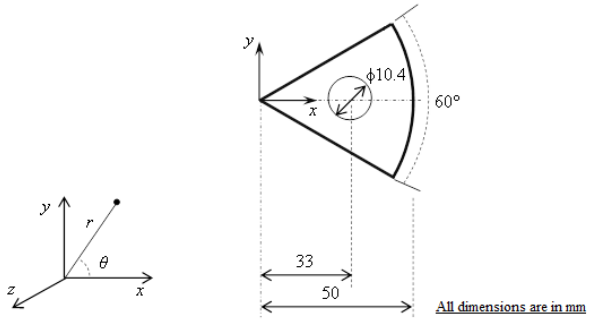

Figure 4 Schematic diagram of the numerical domain

For cylindrical coordinate system, V and $\nabla()$ and $\nabla.()$ are defined as follows:

$$V = u_r e_r + u_\theta e_\theta + u_z e_z$$

$$\nabla.(\ \ ) = \frac{1}{r}\frac{\partial}{\partial r}\left(r(\ \ )\right) + \frac{1}{r}\frac{\partial}{\partial \theta}(\ \ ) + \frac{\partial}{\partial z}(\ \ )$$

$$\nabla(\ \ ) = e_r\frac{\partial}{\partial r}(\ \ ) + e_\theta\frac{\partial}{\partial \theta}(\ \ ) + e_z\frac{\partial}{\partial z}(\ \ )$$

In equations 12-13, ε is defined as $\delta\times$ liquid fraction of PCM. The source terms (S_i, S_{Tf} and S_{Ts}) mentioned in the equations are presented in table 4. In table 4, ΔE in S_{Tf} is defined as,

$\Delta E = 0$ for $T < T_{solidus}$

$= f_l L_{latent}$ for $T_{solidus} \geq T \geq T_{liquidus}$

For a pure material, isothermal phase change occurs, *i.e.* $T_{solidus} = T_{liquidus} = T_m$. When $f_l = 1$, PCM is in fully liquid state, and when $f_l = 0$, PCM is in solid phase. To simulate phase change problem without porosity *i.e.* TES filled with PCM, the momentum equation (equation 11) is solved by taking $\varepsilon = 1$ and $S_z = \rho g \beta_f\left(T_f - T_{ref}\right)$, whereas in the PCM energy equation (equation 12), S_{Tf} is set to $-\frac{\partial(\rho\Delta E)}{dt}$.

Table 4 Source term definitions

Momentum Equation	S_r	$-\frac{\mu}{K}u_r + \frac{\rho C}{\sqrt{K}}\lvert V\rvert u_r$
	S_θ	$-\frac{\mu}{K}u_\theta + \frac{\rho C}{\sqrt{K}}\lvert V\rvert u_\theta$
	S_z	$-\frac{\mu}{K}u_z + \frac{\rho C}{\sqrt{K}}\lvert V\rvert u_z + \rho g\beta_f\left(T_f - T_{ref}\right)$
Energy Equation	S_{Tf}	$h_{sf}a_{sf}\left(T_s - T_f\right) - (1-\delta)\frac{\partial(\rho\Delta E)}{dt}$
	S_{Ts}	$h_{sf}a_{sf}\left(T_f - T_s\right)$

The interfacial surface area a_{sf} and the permeability of the porous matrix (K) in table 4 are determined by taking the following relations given by Fourie and Du Plesis [11].

$$a_{sf} = \frac{3}{d}(3-\psi)(\psi-1) \tag{14}$$

$$K = \frac{\delta^2 d^2}{36(\psi-1)\psi} \tag{15}$$

The relation between d and d_p can be written as [9],

$$\frac{d_p}{d} = \frac{3-\psi}{\psi} \tag{16}$$

The value of d_p is assumed to calculate of d. The tortuosity can be obtained as [11],

$$\psi = 2 + 2cos\left[\frac{4\pi}{3} + \frac{1}{3}\cos^{-1}(2\psi - 1)\right] \tag{17}$$

The drag coefficient is found by the following expression [11],

$$C_{D,f} = 1 + \frac{10}{Re^{0.667}} \tag{18}$$

where, $Re = \frac{\rho U d}{\mu}$ (19)

The inertial coefficient (C) can be written as [11],

$$C = (3-\psi)(\psi-1)\frac{C_{D,f}\psi^{1.5}}{24\delta^2} \tag{20}$$

The effective thermal conductivity (k_e) of porous medium can be determined by [9],

$$k_{eff} = \frac{\left[k_f + \pi\left(\sqrt{\frac{1-\delta}{3\pi}}\frac{1-\delta}{3\pi}\right)(k_s - k_f)\right]\left[k_f + \frac{1-\delta}{3}(k_s - k_f)\right]}{k_f + \left[\frac{4}{3}\sqrt{\frac{1-\delta}{3\pi}}(1-\delta) + \pi\sqrt{\frac{1-\delta}{3\pi}}(1-\delta)\right](k_s - k_f)} \tag{21}$$

The density, specific heat and latent heat of the porous medium are calculated by the volume averaged technique [12],

$$\rho_{eff} = (1-\delta)\rho_s + \delta\rho_f \tag{22}$$

$$(\rho c)_{eff} = (1-\delta)\rho_s c_s + \delta\rho_f c_f \tag{23}$$

$$L_{latent,eff} = \delta L_{latent} \tag{24}$$

The interfacial heat transfer coefficient (h_{sf}) between the PCM and the metal matrix is determined by assuming quasi-steady heat conduction between the porous matrix and the PCM where motion of liquid phase is neglected [9]. The Nusselt number is defined as,

$$Nu = \frac{h_{sf} d_{fi}}{k_f} = \frac{2\left(\frac{k_s}{k_f}\right)}{\ln(1-B) + \left(\frac{k_s}{k_f}\right)\ln(1+A)} \tag{25}$$

For small values of A and B, the relation between A and B is,

$$A = B\sqrt{\frac{\alpha_s}{\alpha_f}} \tag{26}$$

Boundary and Initial Conditions

At $t = 0$, $T(r,\theta,z,0) = 165.9$ °C which is slightly below the T_m.

The boundary conditions are:

i) No slip and impermeability condition at the walls, *i.e.* $u_i = 0$

ii) At inlet, $z = 0$, $u_z = u_{in}$ and $T_z = T_{in}$

iii) At outlet, $z = L$, pressure outlet boundary condition with $p = 0$

iv) Insulated sidewalls and outer surface of the TES at $r = \frac{D_i}{2}$.

v) Symmetric boundary conditions are taken for the symmetry planes at $\theta = 0$ and $\theta = 60°$.

The inlet temperature (T_{in}) of HTF is maintained at 200 °C for 1800 s during charging period and at 132 °C for the same duration during discharging period. A commercial software Fluent 14 is used in the simulations. The governing equations are solved iteratively using finite volume method (FVM) according to the SIMPLE algorithm. Coefficients in the momentum and energy equations are determined by power law. The total number of cells in the domain is chosen as 816070 after the grid independence study. The present numerical model is validated by comparing it with the results reported by Khillarkar et al. [13] for the melting of PCM in an irregular geometry.

RESULTS AND DISCUSSIONS

Numerical study of the thermal performance of TES filled with PCM is performed. The outer and sidewalls of the TES are kept insulated and the TES is initially at 165.9 °C which is lower than the PCM melting temperature of 166 °C. The inlet temperature of heat transfer fluid (HTF) is maintained at 200 ^{0}C for 1800 s during charging period and at 132 ^{0}C for the same duration during discharging period. Figure 6 shows the temperature history of the outlet temperature of HTF. It can be observed from the figure that the HTF outlet temperature increases from its initial temperature and then stabilizes when PCM starts changing its phase. The outlet temperatures of HTF flowing through the centre and outer tubes stabilize at 184.3 ^{0}C and 183.4 ^{0}C after 800 s. The difference in the two outlet temperatures of HTF is due to the arrangement of pipes in the storage system, in which the centre pipe is surrounded and affected by heat transfer from the six outer pipes. Hence the outer tube outlet temperature is lower than that of the centre tube and the maximum temperature difference is found to be 0.9 ^{0}C. Therefore, for the further cases, the HTF outlet temperature of centre tube will be shown. During the discharging period, PCM releases heat to HTF which is at lower temperature than the PCM. There is a sudden temperature drop to 157 ^{0}C within 100 s at the beginning of the discharging period. After that the temperature of HTF gradually reduces and it reaches to 140 °C at 3600 s.

The efficacy of using PCM in TES can be noted from figure 6. This can be shown by using steel as a storage medium that stores the energy in the form of sensible heat. It can be observed from the figure that the outlet temperature of HTF always increases exponentially with time when steel is used as a storage material. After 1800 s, the HTF temperature reaches 197 ^{0}C and similar trend is also observed during discharging period and the temperature reaches 135 ^{0}C at 3600 s. The temperature difference at the end of the melting and the solidification at the outlet of HTF (ΔT) is minimum (44 °C) for the case where PCM is used as the storage material compared to steel (62 °C). Hence it can be concluded that the PCM can effectively stabilizes the temperature fluctuations of the incoming HTF effectively.

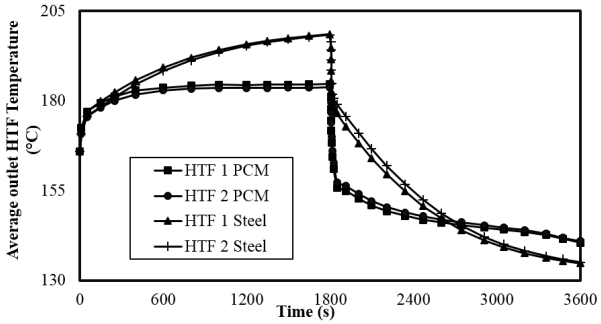

Figure 6 HTF outlet temperature for Steel and PCM as a storage material

Metal matrix and foams are introduced in PCM as thermal conductivity enhancers (TCE) to improve the heat transfer rate. An addition of small amount of TCE of 10% to PCM, which corresponds to the porosity (δ) of 0.9, leads to an enhancement of effective thermal conductivity of the TES. The pore diameter of the metal matrix is taken as 1 mm. The temperature variation of HTF at the pipe outlet with time is plotted for PCM and δ = 0.9 in figure 7. It can be seen from the figure that the outlet temperature of HTF stabilizes at 180.21 °C for δ = 0.9 after 800 s. At the end of the charging process, the average temperature of HTF outlet reaches to 182.42 °C for δ = 0.9. During discharging period, HTF absorbs heat from PCM due to its lower temperature than that of PCM. The temperature drops quickly to 155.98 °C for δ = 0.9 within 50 s at the beginning of the discharging period. Then the temperature of the HTF outlet gradually reduces and it reaches to 147.96 °C for δ = 0.9 at 3600 s. Therefore one can find that the temperature difference (ΔT) at the HTF outlet for TES filled with PCM is much higher (44.24 °C) compared to that with δ = 0.9 (34.46 °C). Hence the fluctuation at the HTF outlet temperature can be smoothened by inserting metal matrix in PCM.

Further, a parametric study is performed to investigate the effect of inserting a metal matrix with different porosities on the temperature and melting fields. The HTF temperature at the pipe outlet with time is plotted for the four cases along with the PCM during charging and discharging period in figure 7. At the end of the charging process, the average temperature of HTF outlet reaches to 194.1, 185.48 and 181.54 °C, respectively for δ = 0.3, 0.5 and 0.7. During discharging period, the HTF outlet temperature reaches to 142.22, 148.5, and 149.17 °C for δ = 0.3, 0.5 and 07, respectively at 3600 s. Therefore it can be found that the temperature difference (ΔT) is high for δ = 0.3 and the same is low for δ = 0.7 compared to others. For δ = 0.7, ΔT is low because one can note that the effective thermal diffusivity of the PCM is maximum at δ = 0.7 as shown in figure 8. However, PCM melts faster in case of δ = 0.3 as the latent heat content of the thermal storage system is low due to the presence of high amount of metal matrix which promotes the conduction heat transfer.

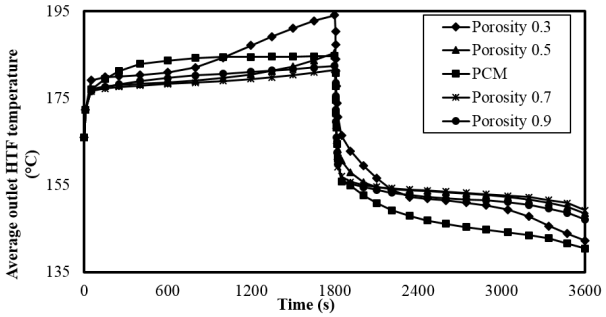

Figure 7 HTF outlet temperature plot for PCM and porosity 0.9, 0.7, 0.5 and 0.3

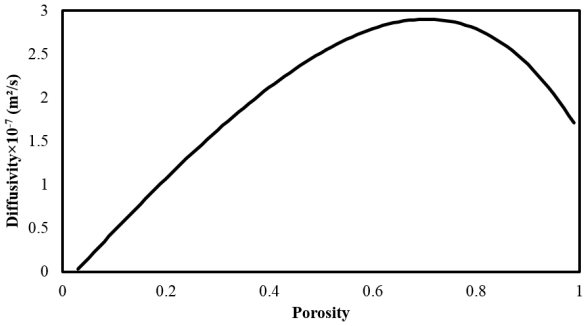

Figure 8 Effective thermal diffusivity *vs.* porosity

CONCLUSION

In this paper, the thermal performance of a thermal energy storage (TES) system using PCM is investigated for the medium temperature application (~ 200 °C) such as ORC based solar thermal power plant. Metal foam and matrix is used as the thermal conductivity enhancers (TCE). A numerical model using enthalpy porosity technique is used to characterize the thermal storage system. The fluctuations in the inlet temperature of HTF are introduced by a cycle consisting of charging and discharging period. The heat transfer enhancement of PCM with TCE in TES is also evaluated and compared with TES filled with PCM. The effect of porosity of metal foam and matrix on the thermal performance of PCM-based TES is investigated. It is found that PCM can be used in more effective way to reduce the fluctuations in the inlet temperature of HTF compared to a sensible heat storage such as steel in this case. Addition of TCE in PCM improves the temperature distribution in PCM, which enhances the heat transfer rate in PCM due to augmentation in the effective thermal conductivity of PCM. The temperature difference is found to be smaller for $\delta = 0.7$ for a given pore diameter which can be attributed to maximum thermal diffusivity. However, PCM melts faster in case of $\delta = 0.3$ as the latent heat content of the thermal storage system is low due to the presence of high amount of metal matrix.

ACKNOWLEDGEMENT

This paper is based on work supported in part under the US-India Partnership to Advance Clean Energy-Research (PACE-R) for the Solar Energy Research Institute for India and the United States (SERIIUS), funded jointly by the U.S. Department of Energy under Subcontract DE-AC36-08GO28308 to the National Renewable Energy Laboratory and the Government of India, through the Department of Science and Technology under Subcontract IUSSTF/JCERDC-SERIIUS/2012 dated 22nd Nov. 2012.

REFERENCES

[1] Sukhatme S.P., Nayak J.K., Solar energy- principles of thermal collection and storage, 3rd Edition, Tata McGraw Hill Education Private Limited, New Delhi, India, 2008.

[2] Calvet N., Olivès R., Bédécarrats J.P., Py X., Dumas J.P., Jay F., Latent heat storage enhancement by thermal conductivity intensification, *In proceedings of EFFSTOCK, the 11th International Conference on Thermal Energy Storage*, Stockholm, Sweden, June 14-17, 2009.

[3] Tay N.H.S., Belusko M., Bruno F., Designing a PCM storage system using the effectiveness-number of transfer units method in low energy cooling of buildings, *Energy and Buildings*, Vol. 50, 2012, pp. 234–242.

[4] Socaciu L.G., Thermal Energy Storage with Phase Change Material*, Leonardo Electronic Journal of Practices and Technologies*, Vol. 20, January-June 2012, pp. 75-98.

[5] Trelles J.P., Duflyv, Numerical simulation of porous latent heat thermal energy storage for thermoelectric cooling, *Applied Thermal Engineering*, Vol. 23, 2003, pp. 1647–1664.

[6] Mettawee E.S., Assassa G.M.R., Thermal conductivity enhancement in a latent heat storage system, *Solar Energy*, Vol. 81, 2007, pp. 839–845.

[7] Felix Regin A., Solanki S.C., Saini J.S., Heat transfer characteristics of thermal energy storage system using PCM capsules: A review, *Renewable and Sustainable Energy Reviews*, Vol. 12, 2008, pp. 2438–2458.

[8] Sciacovelli A., Verda V., Gagliardi F., Thermo-fluid dynamic model for control analysis of latent heat thermal storage system, *Proceedings of ECOS 2012- the 25th International Conference on Efficiency, Cost, Optimization, Simulation and Environmental Impact of Energy Systems*, June 26-29, 2012, ITALY.

[9] Mesalhy O., Lafdi K., Elgafy A., Bowman K., Numerical study for enhancing the thermal conductivity of phase change material (PCM) storage using high thermal conductivity porous matrix, *Energy conservation and Management*, Vol. 46, 2005, pp. 847-867.

[10] Brent A.D., Voller V.R., Reid K.J., Enthalpy-porosity technique for modeling convection-diffusion phase change: Application to the melting of a pure metal, *Numerical Heat Transfer*, Vol. 13, 1988, pp. 297-318.

[11] Fourie J.G., Du Plessis J.P., Pressure drop modelling in cellular metallic foams, Chemical Engineering Science, Vol. 57, 2002, pp. 2781 – 2789.

[12] Nayak K.C., Saha S.K., Srinivasan K., Dutta P., A numerical model for heat sinks with phase change materials and thermal conductivity enhancer, *International Journal of Heat and Mass Transfer*, Vol. 49, 2006, pp. 1833-1844.

[13] Khillarkara D.B., Gongb Z.X., Mujumdara A.S., Melting of a phase change material in concentric horizontal annuli of arbitrary cross-section, *Applied Thermal Engineering*, Vol. 20, 2000, pp. 893 - 912.